International Immunopharmacology 66 (2019) 146–153

Contents lists available at ScienceDirect

International Immunopharmacology

journal homepage: www.elsevier.com/locate/intimp

Epicatechin alleviates inflammation in lipopolysaccharide-induced acute lung injury in mice by inhibiting the p38 MAPK signaling pathway

Jing Xing[a,b], Zhenlong Yu[c], Xiangyu Zhang[d], Wenyang Li[a], Dongna Gao[b], Jian Wang[d], Xiaochi Ma[c], Xinshi Nie[a], Wei Wang[a,*]

[a] Respiratory and Critical Care Department, The First Hospital of China Medical University, Shenyang, Liaoning, China
[b] Emergency Department, The First Affiliated Hospital of Dalian Medical University, Dalian, Liaoning, China
[c] Academy of Integrative Medicine, College of Pharmacy, Dalian Medical University, Dalian, Liaoning, China
[d] Key Laboratory of Structure-based Drug Design & Discovery, Ministry of Education, Shenyang Pharmaceutical University, Shenyang, Liaoning, China

ARTICLE INFO

Keywords:
ALI
LPS
Epicatechin
p38
AP1

ABSTRACT

The p38 MAPK signaling pathway plays a key role in lung inflammation and the development of acute lung injury (ALI). We previously reported that the phenolic compound procyanidin B1 inhibits inflammation by suppressing the p38 MAPK signaling pathway. Here, we asked whether the monomer of procyanidin B1, epicatechin (EC), can alleviate LPS-induced ALI in mice, and if so, whether EC acts by inhibiting p38 MAPK. C57BL/6 mice were randomly divided into four groups (n = 8) and received EC alone, vehicle (sham group), LPS alone, or LPS and EC. LPS was administered via intraperitoneal injection and EC via nasogastric feeding. Lung histopathology, alveolocapillary membrane permeability, inflammation, and p38 MAPK pathway activation were assessed by immunohistochemistry, tissue wet/dry weight analysis, quantitative PCR, protein assays, ELISA, and western blot analysis using lung tissue and/or bronchoalveolar fluid. We also performed molecular modeling and in vitro enzymatic assays to examine the potential interaction between EC and p38 MAPK at the molecular level. We found that LPS caused an increase in ALI-associated lung pathology accompanied by activation of p-p38 pathway components and the transcription factor AP1. All of these effects were substantially reduced by treatment with EC. Furthermore, molecular modeling suggested that EC suppressed p38 MAPK signaling by hydrogen bonding with Glu71, Ala 111, Asp112, and Leu171 in the active site of p38α. In vitro kinase assays confirmed the ability of EC to directly inhibit purified p38 MAPK. Collectively, our data suggest that the naturally occurring compound EC could be a new therapeutic option for ALI.

1. Introduction

The pathophysiology of acute lung injury (ALI) is characterized by acute inflammation of the lungs, with increased pulmonary vascular permeability, alveolar septal edema, and alveolar endothelial cell and epithelial cell injury [1]. ALI can be induced by multiple events that dysregulate normal inflammatory and anti-inflammatory responses, resulting in upregulated production of pro-inflammatory mediators with subsequent tissue damage. In recent years, anti-inflammatory therapies have been developed that show an improved ability to alleviate the rapid progression of lung injury [2,3].

Many features of human ALI can be recapitulated in animal models by administration of LPS [4]. LPS activates inflammatory responses by binding to Toll-like receptors expressed on immune cells, thereby triggering signaling via multiple pro-inflammatory pathways such as the p38 MAPK pathway. In turn, p38 MAPK activates downstream transcription factors such as NF-κB and AP-1 [5], which induce the production of a large number of inflammatory mediators, including cytokines and chemokines.

Epicatechin (EC), a monomer of the phenolic compound procyanidin B1, is one of several recently described anti-inflammatory interventions that may be beneficial in alleviating the rapid progression of tissue damage [6,7]. EC is abundant in common cereals, vegetables, and fruits, and it has a wide range of physiological activities [8]. While the antioxidant effect of EC is well known, its anti-inflammatory effects remain enigmatic. We previously showed that procyanidin B1 inhibits inflammation by suppressing activation of p38 MAPK signaling [9], suggesting the possibility that EC may also have beneficial effects on

* Corresponding author at: Respiratory and Critical Care Department, Institute of Respiratory Disease, The First Hospital of China Medical University, 155 Nanjing North Street, Heping District, Shenyang 110001, Liaoning, China.
E-mail address: wwbycmu@126.com (W. Wang).

https://doi.org/10.1016/j.intimp.2018.11.016
Received 15 September 2018; Received in revised form 8 November 2018; Accepted 11 November 2018
Available online 16 November 2018
1567-5769/

inflammation [10]. Indeed, EC has been shown to prevent LPS-induced renal inflammation in vivo [11]. Current evidence indicates that EC suppresses activation of pro-inflammatory pathways and prevents excessive inflammatory responses [12]. However, it is not known whether EC inhibits inflammation in ALI or whether it can suppress p38 MAPK pathway activation in the lung.

Here, we investigated the effects of EC in mice with LPS-induced ALI. We found that EC does indeed alleviate inflammatory lung injury and that the underlying molecular mechanism includes inhibition of p38 MAPK activity, possibly via direct binding of EC to the active site, and consequent suppression of the pro-inflammatory transcription factor AP1.

2. Materials and methods

2.1. Mice

Pathogen-free C57BL6/N mice (male, 6–8 weeks old, 20.5 ± 2.5 g) were obtained from the Beijing Vital River Laboratory Animal Technology Co. Ltd. (Beijing, China; certificate number 11400700225788). The experimental protocol was approved by the Committee on the Ethics of Animal Experiments of China Medical University, and mice were handled in accordance with the China Medical University guide for animal care and use of laboratory animals. Animals were housed in an environment controlled for temperature (23 °C), humidity (50%), and light (12 h dark-light cycles). Mice were allowed free access to aseptic chow and water and were acclimated for 1 week before experiments.

2.2. Model of LPS-induced ALI and EC treatment

A total of 32 mice were randomly divided into four groups of 8 mice: (1) The EC group was administered 5 ml/kg of normal saline (NS) by intraperitoneal (IP) injection at time 0, followed by 15 mg/kg (5 ml/kg) of EC (Aladdin, Shanghai, China; HPLC purity ≥98.0%) by nasogastric feeding 30 min and 12 h later. (2) The sham (vehicle) group was administered 5 ml/kg NS by IP injection at time 0, followed by administration of the same volume of NS by nasogastric feeding 30 min and 12 h later. (3) The LPS group was administered 10 mg/kg of LPS (*Escherichia coli*, 055:B5; Sigma, St. Louis, MO, USA; 2 mg/ml in NS) by IP injection at time 0, followed by 5 ml/kg of NS by nasogastric feeding 30 min and 12 h later. (4) The LPS + EC group was administered 10 mg/kg of LPS by IP injection at time 0, followed by 15 mg/kg of EC by nasogastric feeding 30 min and 12 h later. The dosing and delivery regimen for EC were selected based on previous work by others [11,13–16] as well as our preliminary studies [17]. At 24 h post-treatment, mice were sacrificed under anesthesia and lung tissues and bronchoalveolar fluid (BALF) were collected. ALI was confirmed by histological evidence of lung tissue injury, alteration of the alveolar capillary barrier, and the presence of an inflammatory response [18].

2.3. Lung analyses

The right lower lungs were collected, rinsed with cold NS, fixed with 4% formaldehyde for 24 h, and embedded in paraffin. The tissue blocks were then cut into 3-μm-thick sections and stained by standard procedures with hematoxylin and eosin (H&E; Beijing Coribo Technology Co. Ltd., Beijing, China) for histological analysis. A lung injury score was assigned based on five parameters according to the American Thoracic Society workshop guidelines [18]: (A) neutrophil abundance in the alveolar space, (B) neutrophil abundance in the interstitial space, (C) hyaline membranes, (D) proteinaceous debris filling the airspace, and (E) alveolar septal thickening. The ALI score was calculated as $[(20 \times A) + (14 \times B) + (7 \times C) + (7 \times D) + (2 \times E)] / (\text{number of fields} \times 100)$. Alveolar septal thickening was measured as previously described [19]. The ratio of alveolar septal thickness from mice in the sham group was set as 1.

The moisture content of the accessory lobes of the right lungs was calculated from the ratio of wet/dry weight. The tissue surface was blotted dry with filter paper, placed in an EP pipe, and weighed. The pipes were then incubated at 60 °C for 72 h to remove all moisture, the dry weights were recorded, and the wet/dry weight ratio was calculated.

2.4. BALF analyses

After sacrifice, the left lungs were immediately lavaged twice with 0.5 ml of ice-cold NS via a catheter. The BALF was collected (volume recovery rate > 80%), and the absolute number of neutrophils present was measured using an XN-1000 hematology analyzer (Sysmex Corp., Shanghai, China). For analysis of protein content, BALF samples were centrifuged at 1500 rpm for 10 min at 4 °C, and the supernatants were collected and stored at −80 °C until assayed. Total protein content was measured with an enhanced BCA protein assay kit (Beyotime Biotechnology, Shanghai, China) according to the manufacturer's instructions. Absorbance at 562 nm was measured using a plate reader (BioTek Instruments Inc., Winooski, VT, USA).

2.5. Enzyme-linked immunosorbent assay (ELISA)

The concentration of IL-6 protein in BALF samples was measured by ELISA according to the manufacturer's instructions (Meimian Industrial Co. Ltd., Yancheng, Jiangsu, China). Absorbance at 450 nm was measured using a plate reader (BioTek Instruments Inc.).

2.6. Quantitative RT-PCR

Total RNA was isolated from the lung tissues using an RNeasy Mini Kit and an RNase-Free DNase Set (Qiagen, Hilden, Germany) according to the manufacturer's protocol. Complementary DNA (cDNA) was synthesized from total RNA using an RT2 First Strand Kit (Qiagen) according to the manufacturer's protocol. cDNA was amplified using a 7500 Real-Time PCR System (Applied Biosystems, Foster City, CA, USA) using the following sequence-specific primers (designed and synthesized by Takara Biotechnology): TNF-α 5′-GCCAGGAGGGAGAACAGAAACTC-3′ (sense) and 5′-GGCCAGTGAGTGAAAGGGACA-3′ (antisense), c-Jun 5′-ATCCACGGCCAACATGCTC-3′ (sense) and 5′-ACGTTTGCAACTGCTGCGTTAG-3′ (antisense), β-actin 5′-CATCCGTAAAGACCTCTATGCCAAC-3′ (sense) and 5′-ATGGAGCCACCGATCCACA-3′ (antisense), IL-6 5′-CCACTTCACAAGTCGGAGGCTTA-3′ (sense) and 5′-TGCAAGTGCATCATCGTTGTTC (antisense). Relative mRNA expression was determined after normalizing to β-actin levels using the 2ΔCt method. mRNA levels from mice in the sham group were set as 1.

2.7. Western blot analysis

The upper lobes of the right lungs were preserved in liquid nitrogen until they were homogenized in lysis buffer (Beyotime Biotechnology) containing a phosphatase inhibitor cocktail (Biotool, Houston, TX, USA). Homogenized samples were subjected to SDS-PAGE and transferred to polyvinylidene difluoride membranes. After blocking, the membrane was probed with primary antibodies specific for TNF-α (1:1000), p38 (1:1000), phospho (p)-p38 (1:1000), c-Jun (1:1000), p-c-Jun (1:1000), and glyceraldehyde 3-phosphate dehydrogenase (GAPDH; 1:4000), all obtained from Cell Signaling Technology (Danvers, MA, USA). The blots were then washed three times with TBST and incubated with a horseradish peroxidase-conjugated secondary antibody (1:5000, Cell Signaling Technology) for 2 h at room temperature. Proteins were detected using ECL reagent (GE Healthcare, Little Chalfont, Buckinghamshire, UK). Immunoreactive bands were photographed using an imaging system (Bio-Rad) and quantified using ImageJ software (National Institutes of Health, Bethesda, MD, USA).

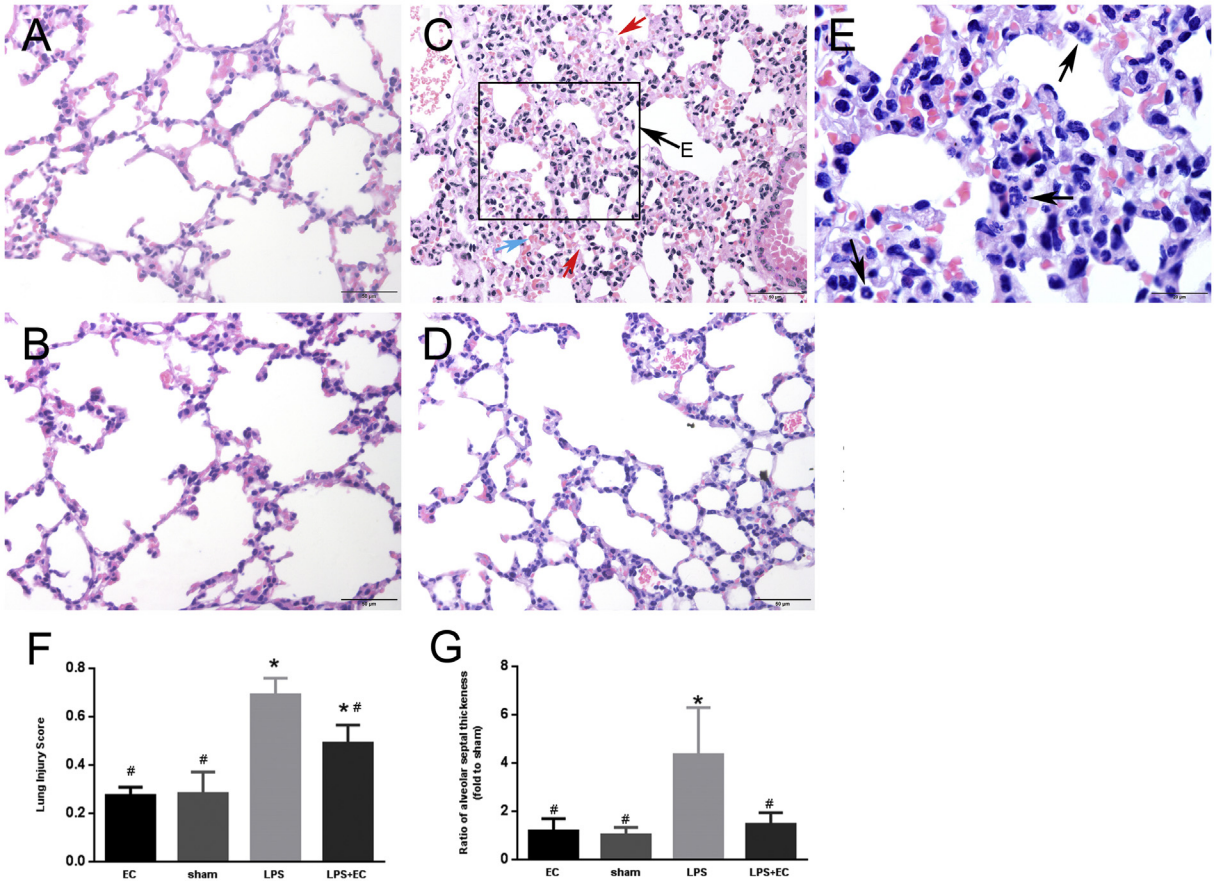

Fig. 1. Epicatechin alleviates lung damage in mice with LPS-induced ALI. (A–D) H&E staining of lung sections from representative mice in the EC (A), sham (B), LPS (C), and LPS + EC (D) groups at 24 h (n = 8 mice/group). Scale bars, 50 μm. Red and blue arrows in (C) indicate proteinaceous debris and hemorrhagic changes, respectively. (E) Magnified image of the black box shown in panel (C). Scale bar, 20 μm. Black arrows indicate neutrophils in the alveolar and interstitial spaces. (F, G) Quantification of histopathologic damage as assessed by the lung injury score (F) and the ratio of alveolar septal thickness (G) at 24 h after the indicated treatments. Values are means ± SD of 8 mice/group. $*P < 0.05$ vs. the sham group, $\#P < 0.05$ vs. the LPS group. (For interpretation of the references to colour in this figure legend, the reader is referred to the web version of this article.)

TNF-α, p-p38/p38, total p38, total c-Jun, and p-c-Jun expression levels were normalized to GAPDH levels.

2.8. Immunohistochemistry

The right lower lungs were fixed in 4% formaldehyde for 24 h and embedded in paraffin. Tissue sections were cut (4 μm thick) and then stained using an SP Kit (XSGB-Bio, Beijing, China) according to the manufacturer's protocol. The primary antibody was anti-p-p38 (1:200, Affinity Biosciences, Cincinnati, OH, USA) and was added for 24 h at 4 °C. Colour development was achieved with a Universal Detection DAB-kit (ZSGB-BIO, Beijing, China) according to the manufacturer's instructions. Finally, the sections were analyzed on a BX53 microscope (Olympus, Tokyo, Japan) and images were captured with an Olympus DP73 camera.

2.9. Molecular docking of EC and p38α (4L8M)

The X-ray crystallographic structure of p38α obtained from the Protein Data Bank (http://www.rcsb.org/pdb) was used in docking calculations (PDB code: 4L8M, 2.1 Å resolution). p38 and EC structures were built and minimized with Accelrys Discovery Studio 3.0 software package, which involved removing the ligand and crystallographic water molecules from the protein and adding hydrogens. With the "Create Pharmacophore Automatically" tool in the "Pharmacophores" module of Discovery Studio 3.0, we selected the protein and EC as the "Receptor" and "Ligand," respectively, in the option "Receptor-Ligand Pharmacophore Generation." The ligand-based pharmacophore model was applied to identify the privileged structure and binding site of 4L8M. X-scores were utilized to predict the binding free energies of EC complexing with 4L8M.

2.10. In vitro p38α enzymatic assay

Kinase reaction buffer (10 mM $MgCl_2$, 1 mM $MnCl_2$, and 1 mM dithiothreitol in enzymatic buffer; Cisbio, Provence, France) was mixed with ATF2, EC, ATP (all from Sigma), and p38α protein kinase (Carna Biosciences Inc., Kobe, Japan) to give final concentrations of 1 μM, 40 μM, 25.1 μM, and 1 μg/ml, respectively. The mixture was centrifuged at low speed and pre-incubated for 60 min at room temperature. Anti-GST-XL665 (0.5 μM; Cisbio) and anti-p-ATF-2 (Thr71)-cryptate (0.9 μg/ml; Cisbio) were then added to the reaction, and the incubation was continued at room temperature for an additional 120 min. Negative and positive controls consisted of the same reactions in the absence of EC and in the presence of staurosporine (Selleck, Shanghai, China), respectively. Fluorescence was measured using a multimode reader (Tecan, Hombrechtikon, Switzerland) at 620 nm (for cryptate) and 665 nm (for XL665). The ratio of absorbance at 665/620 for each reaction was calculated. Data were analyzed using Prism 5.0 (GraphPad Software Inc., San Diego, CA, USA).

2.11. Statistical analysis

Statistical analyses were performed using SPSS version 16.0 (SPSS

Inc., Chicago, IL, USA). Data are presented as the mean ± SD. Differences were compared using one-way analysis of variance followed by either Fisher's least significant difference test for multiple comparisons (when homogeneity of variance was assumed) or Dunnett's T3 test (when heterogeneity of variance was assumed). $P < 0.05$ was considered statistically significant.

3. Results

3.1. EC alleviates lung damage in mice with LPS-induced ALI

To determine whether EC treatment could reduce lung damage induced by LPS, groups of mice were injected IP with vehicle or LPS and treated nasogastrically with EC or vehicle at time 0, 0.5 h, and 12 h. After 24 h, the mice were sacrificed and the lungs were removed, sectioned, and stained with H&E. As shown in Fig. 1A and B, the lung tissue of animals administered EC alone showed no significant histological changes compared with sham-treated animals. In contrast, the lung tissue from animals injected with LPS was discontiguous, with neutrophils present in the alveolar and interstitial spaces, hyaline membranes, and proteinaceous debris filling the airspace (Fig. 1C, E). Moreover, the alveolar septum was more than four times thicker than normal (Fig. 1G), and alveolar hemorrhage and structural damage could also be observed (Fig. 1C). Notably, the severity of LPS-induced histopathologic lung damage was significantly reduced in animals treated with EC compared with vehicle (Fig. 1D). Quantification of the lung injury confirmed that EC treatment had no effect on the control animals but significantly decreased the scores of the LPS group (Fig. 1F).

3.2. Epicatechin reduces alveolocapillary membrane permeability in mice with LPS-induced ALI

To evaluate the effects of LPS and EC on alveolocapillary membrane permeability and lung edema, we measured the protein concentration in BALF and the ratio of wet to dry lung weights [18]. As shown in Fig. 2, the protein and moisture content were significantly higher in the lungs of LPS-treated compared with sham-treated mice after 24 h. However, treatment with EC significantly reduced both parameters to the levels observed in sham-treated mice (Fig. 2). These data indicate that EC effectively prevents the LPS-induced increase in vascular permeability.

3.3. Epicatechin reduces the lung inflammatory response in mice with LPS-induced ALI

Next, we measured the LPS-induced inflammatory response by quantifying infiltrating neutrophils in BALF, TNF-α mRNA and protein levels in lung tissue, IL-6 mRNA levels in lung tissue, and IL-6 protein levels in BALF. As shown in Fig. 3A, we observed a marked increase in neutrophil numbers in BALF from LPS-challenged mice, but this was completely blocked by co-treatment with EC. Similarly, qRT-PCR analysis showed that LPS administration induced a significant increase in TNF-α and IL-6 mRNA levels in lung tissue, and this was significantly inhibited by EC (Fig. 3B, D). Finally, western blot and ELISA analyses revealed a significant increase in TNF-α and IL-6 protein levels in the lung tissue and BALF, respectively, of LPS-treated mice, and this too was significantly inhibited by EC (Fig. 3C, E).

3.4. Epicatechin reduces LPS-induced p38 MAPK phosphorylation in the lungs of mice with LPS-induced ALI

To determine whether the protective effects of EC in LPS-challenged mice are mediated via the p38 MAPK significant pathway, we performed western blot analysis of total and active (phosphorylated) enzyme in lung tissue. We observed that levels of phosphorylated p38, but not total p38, were increased in lung tissues from the LPS and LPS + EC-treated groups, but the increase was significantly smaller in the LPS + EC group (Fig. 4A). To corroborate this finding, we examined the distribution of p-p38 in lung sections by immunohistochemistry. As shown in Fig. 4Dp-p38 staining was more intense in the alveolar epithelial cells, vascular endothelial cells, and inflammatory cells of lung sections from LPS-treated mice compared with the sham-treated mice (Fig. 4C). Consistent with the western blot and immunohistochemistry analyses, the expression of p-p38 was significantly lower in the LPS + EC group compared with the LPS group (Fig. 4E). Taken together, these results indicate that EC significantly inhibits the expression of active p38 in the lung tissue of mice with LPS-induced ALI.

3.5. Molecular modeling and enzymatic assays support direct binding of EC to p38α

Next, we examined the possibility that EC may inhibit p38 activation by directly binding to the enzyme. Since p38α is the main functional subunit of p38 MAPK and is widely expressed in all tissues, we performed molecular docking modeling using the PDB 4L8M crystal structure of p38 [20]. Fig. 5A and B show the 3-D models of EC and p38 4L8M, with EC fitted into the binding pocket of p38α (surface interaction relationship). The 2-D structures are shown in Fig. 5C. EC appears to bind within the active site pocket of p38α (4L8M) by forming four hydrogen bonds with Glu71, Ala 111, Asp112 and Leu171 (Fig. 5C, D). The ligand–protein binding energy is −8.92 kcal/mol.

To verify the modeling data, we examined the ability of EC to directly inhibit p38 MAPK enzyme activity in vitro. The results showed that EC did indeed inhibit p38α MAPK phosphorylation of its substrate ATF2, a bZIP transcription factor, with an IC_{50} of 2.4 μM (data not shown). Thus, EC can effectively inhibit p38α kinase activity, most likely by direct binding to the enzyme active site.

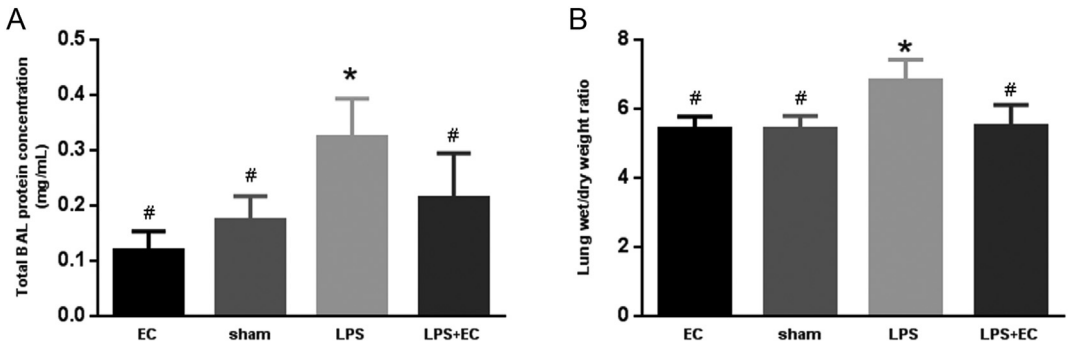

Fig. 2. EC reduces alveolocapillary membrane permeability in mice with LPS-induced ALI. (A, B) Effects of EC on total protein concentration in BALF (A) and lung wet/dry weight ratio (B) at 24 h after the indicated treatments. Values are means ± SD of 8 mice/group. *$P < 0.05$ vs. the sham group, #$P < 0.05$ vs. the LPS group.

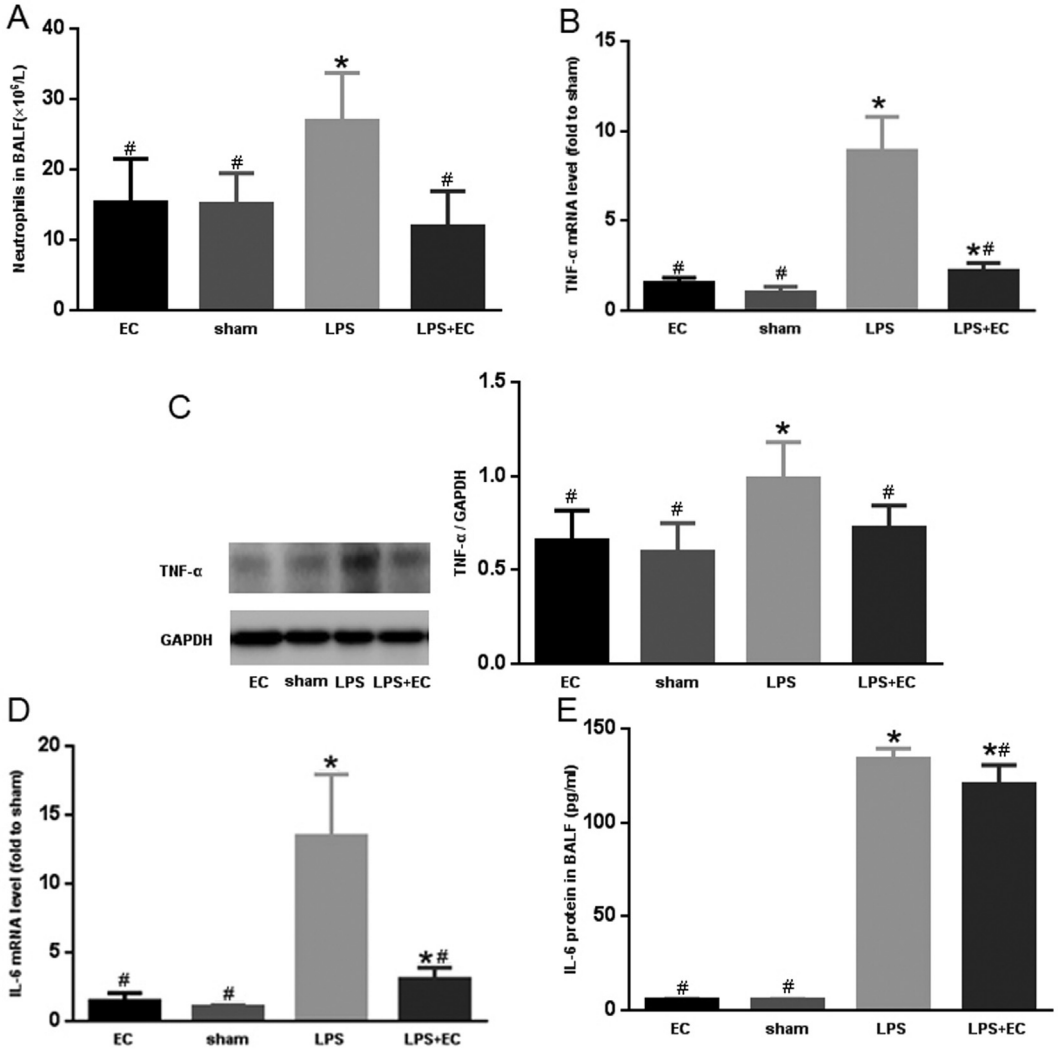

Fig. 3. Epicatechin reduces the lung inflammatory response in mice with LPS-induced ALI. (A–E) Neutrophil numbers in BALF (A), qRT-PCR analysis of TNF-α mRNA in lung tissues (B), western blot analysis (left) and quantification (right) of TNF-α protein in lung tissues (C), qRT-PCR analysis of IL-6 mRNA in lung tissues (D), and ELISA analysis of IL-6 protein level in BALF (E) collected at 24 h after the indicated treatments. Values are the mean ± SD of 8 mice/group. *$P < 0.05$ vs. the sham group, #$P < 0.05$ vs. the LPS group.

3.6. Epicatechin inhibits expression of the transcription factor AP-1 in the lungs of mice with LPS-induced ALI

Finally, we examined the functional consequences of p38 MAPK inhibition by EC in the lungs of mice with ALI. The transcription factor AP-1 comprises multiple Fos (e.g., c-Fos, Fra1) and Jun (e.g., c-Jun, JunB) family proteins that act as homodimers or heterodimers. To assess AP1 expression in lung tissue, we analyzed c-Jun mRNA expression by qRT-PCR. We found that the levels were significantly increased at 24 h after LPS administration compared with sham-treated mice (Fig. 6A). Notably, however, EC treatment reduced c-Jun levels to those observed in the control group (Fig. 6A). Similar results were obtained when we analyzed total and phosphorylated c-Jun protein levels by western blot analysis of lung tissues. As shown in Fig. 6B, LPS increased the expression of both total c-Jun and p-c-Jun, and the increases were virtually abolished by co-treatment with EC. These data demonstrate EC may inhibit production of inflammatory mediators in the lungs of mice with ALI by blocking p38 MAPK-mediated activation of AP1.

4. Discussion

This study provides new evidence that EC can alleviate lung inflammation and play a protective role in ALI induced by an extrapulmonary insult. Previous work has shown that EC can attenuate allergy symptoms and reduce lung inflammation by regulating allergen-specific serum IgE concentrations and inhibiting cyclo-oxygenase 2 expression and nitric oxide production [6,7,21]. Our results extend these data by showing that EC reduces disruption of the alveolar capillary barrier, decreases histological evidence of lung injury, and inhibits the expression of TNF-α and IL-6 in mice with LPS-induced ALI. EC has been shown to inhibit various signaling steps leading to activation of NF-κB [22,23]. Here, we report the novel finding that EC also suppresses p38 MAPK–AP1 signaling, possibly by direct interaction with p38α. Thus EC appears to inhibit inflammation via effects on multiple pro-inflammatory signaling cascades.

Uncontrolled transmigration of neutrophils into the alveolar space and septum is a prominent characteristic of ALI and acute respiratory syndrome [24]. In our study, LPS challenge led to increased alveolo-capillary membrane permeability and an increase in the abundance of neutrophils in BALF, alveolar spaces, and interstitial spaces. However, all of these features were alleviated in the lungs of mice that received EC, indicating that EC can reduce the recruitment and accumulation of neutrophils in the lung during inflammation. Another prominent characteristic of ALI is the production of inflammatory cytokines such

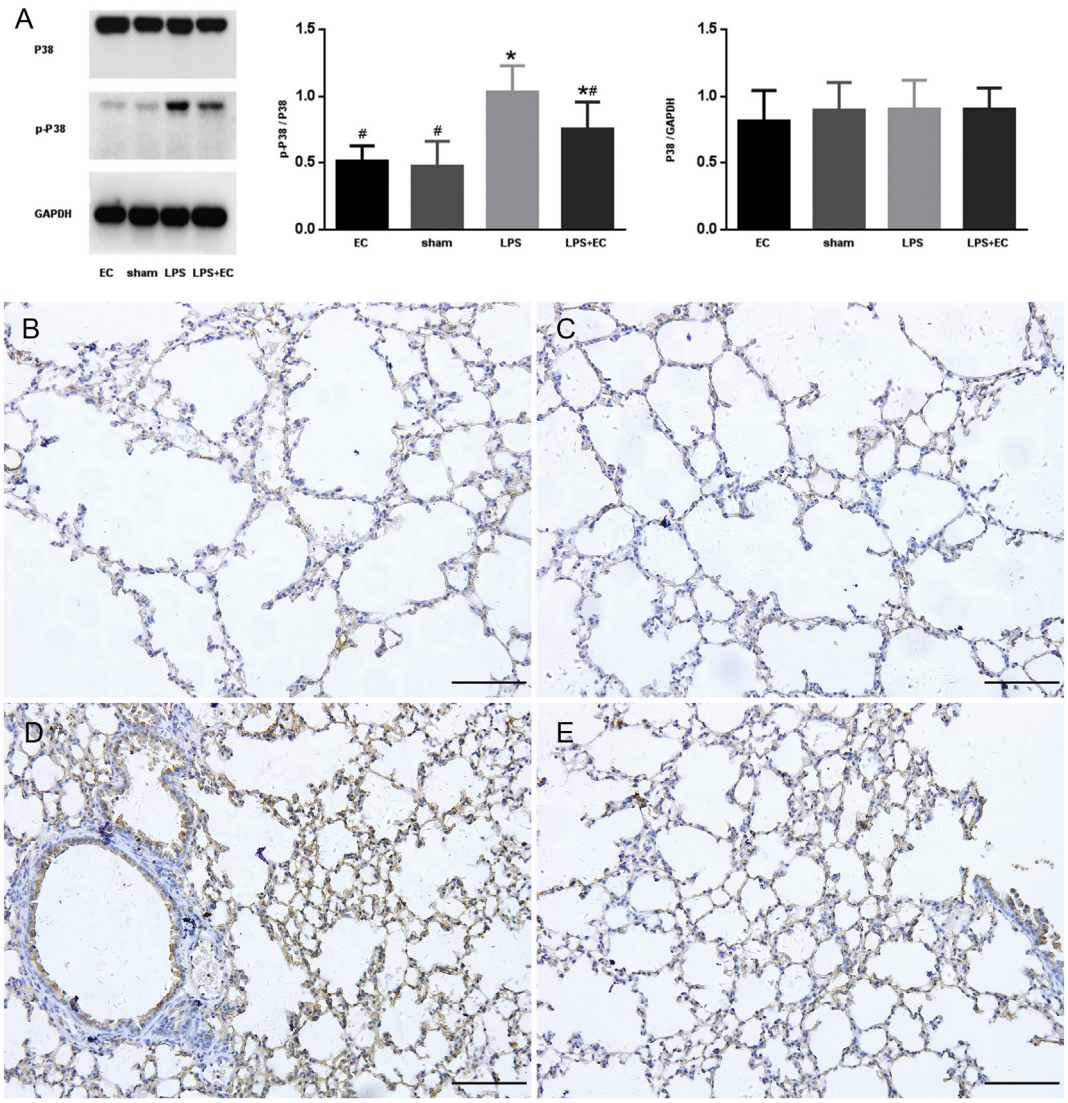

Fig. 4. Epicatechin reduces the expression of phosphorylated p38 in lung tissue from mice with LPS-induced ALI. (A) Western blot analysis (left) and quantification (right) of total p38 and phosphorylated p38 (p-p38) protein levels in lung tissue collected at 24 h after the indicated treatments. (B–E) Immunohistochemical analysis of p-p38 in lung tissue from the EC (B), sham (C), LPS (D), and LPS + EC (E) groups collected at 24 h after the indicated treatments. Scale bars, 100 μm. Values are the mean ± SD of 8 mice/group. *$P < 0.05$ vs. the sham group, #$P < 0.05$ vs. the LPS group.

as TNF-α and IL-6, which are two of the most important pro-inflammatory cytokines. Our results showed that EC significantly suppressed TNF-α and IL-6 production in the lung, further substantiating the anti-inflammatory activity of EC.

The p38 MAPK signaling pathway is known to be activated during LPS-induced ALI [25]. This pathway plays a critical role in regulating neutrophil chemotaxis and TNF-α production in vivo and in vitro [26,27], which is consistent with our finding that EC downregulated the expression of p-p38 in lung tissue as well in addition to reducing neutrophil infiltration. The effects of EC on the p38 MAPK pathway have been examined in only a few studies. For instance, EC was shown to inhibit the expression of α-smooth muscle actin by inhibiting p38 phosphorylation in hepatic stellate cells [28]. In addition, in 3T3-L1 adipocytes cells, EC prevented TNFα-induced expression of inflammatory mediators by inhibiting p38 MAPK–AP1 signaling [29]. However, the mechanism by which EC inhibits p38 MAPK activity is still unclear. It has been reported that EC can be absorbed as a monomer in the gastrointestinal tract [30] and can directly cross cellular membranes to exert its effects [22]. Here, we speculated that EC may regulate p38 MAPK by directly interacting with the protein. The p38 protein family includes p38α, p38β, p38γ (ERK6, SAPK3), and p38δ (SAPK4) [31]. p38α is the main functional subunits and is also referred to as p38. Baur et al. reported the X-ray crystallographic structure of p38α complexed with inhibitors [20]. Here, we performed molecular docking modeling and found that EC could potentially interact with p38α through hydrogen bonding to Ala111, Glu71, Leu171, and Asp112 in the catalytic pocket of p38α. We confirmed this relationship by measuring p38α enzymatic activity with ATF2 as the substrate in vitro and identifying an IC_{50} of 2.4 μM for EC. Thus, one of the major findings of this study is the identification of a potential molecular mechanism for inhibition of p38α by EC and its confirmation in an enzymatic assay in vitro.

The p38 MAPK pathway activates AP1 to regulate transcription of TNF-α [32,33]. Our results show that EC inhibits the expression of total c-Jun and p-c-Jun in the lungs of LPS-challenged mice. This finding suggests that EC may inhibit TNF-α production in the lungs via the p38 MAPK–AP1 signaling pathway.

In conclusion, this study demonstrates the protective effects of EC on LPS-induced ALI in mice. EC inhibits inflammatory injury by inhibiting activation of the p38 MAPK–AP1 signaling pathway, possibly by directly binding to the active site of p38 and inhibiting its catalytic activity.

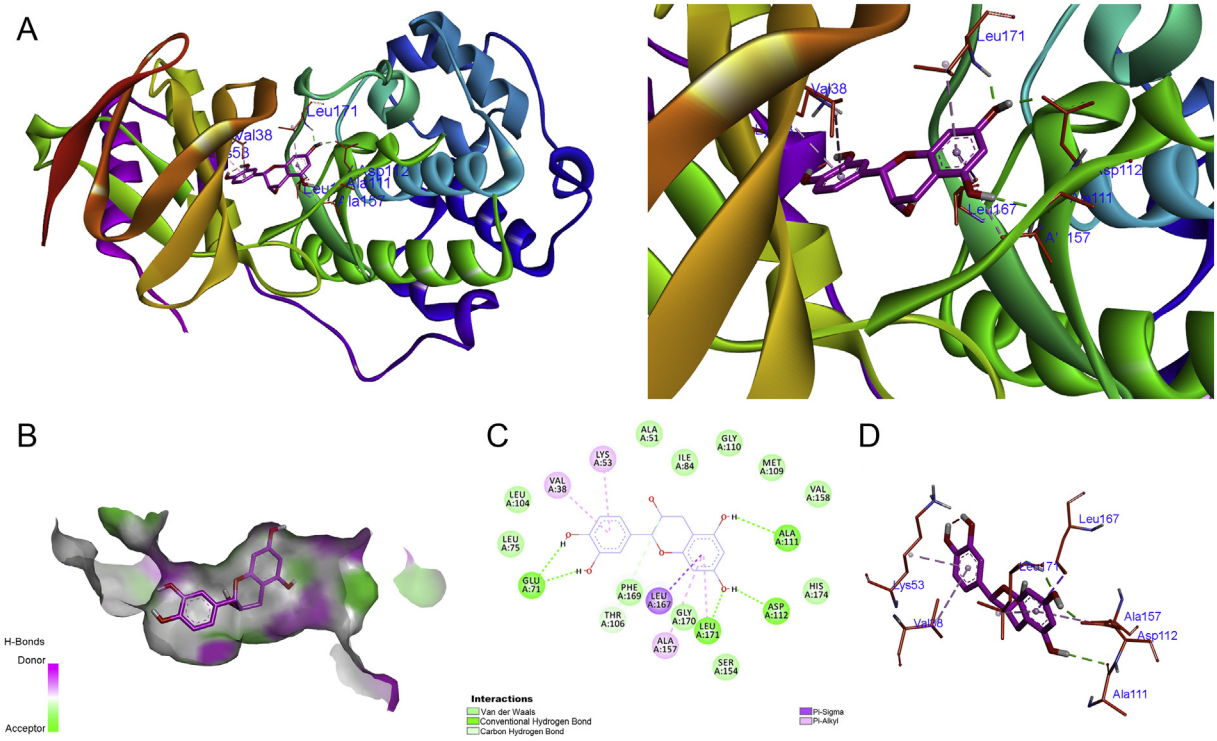

Fig. 5. Modeling of epicatechin binding to p38α (4L8M). (A) 3-D structure of EC in the catalytic domain (Pharmacophore_04) of p38α. (B) Surface interaction relationship between EC and the binding pocket of p38α. (C) 2-D structure of EC and the catalytic domain of p38α. (D) Hydrogen bonding (dashed green lines) between EC and Glu71, Ala 111, Asp112, and Leu171 in the catalytic domain of p38α. (For interpretation of the references to colour in this figure legend, the reader is referred to the web version of this article.)

Acknowledgements

This work was supported by grants from the National Natural Science Foundation of China (81670085) and the Natural Science Foundation of Liaoning Province (20170540295). We are grateful to the Key Clinical Laboratory of Integrated Medicine at the First Affiliated Hospital of Dalian Medical University and the College of Pharmacy at Dalian Medical University for providing laboratory facilities.

Disclosures

No financial relationships or conflicts of interest relevant to this article are declared by the authors.

Conflict of interest

The authors have no financial relationships or conflicts of interest

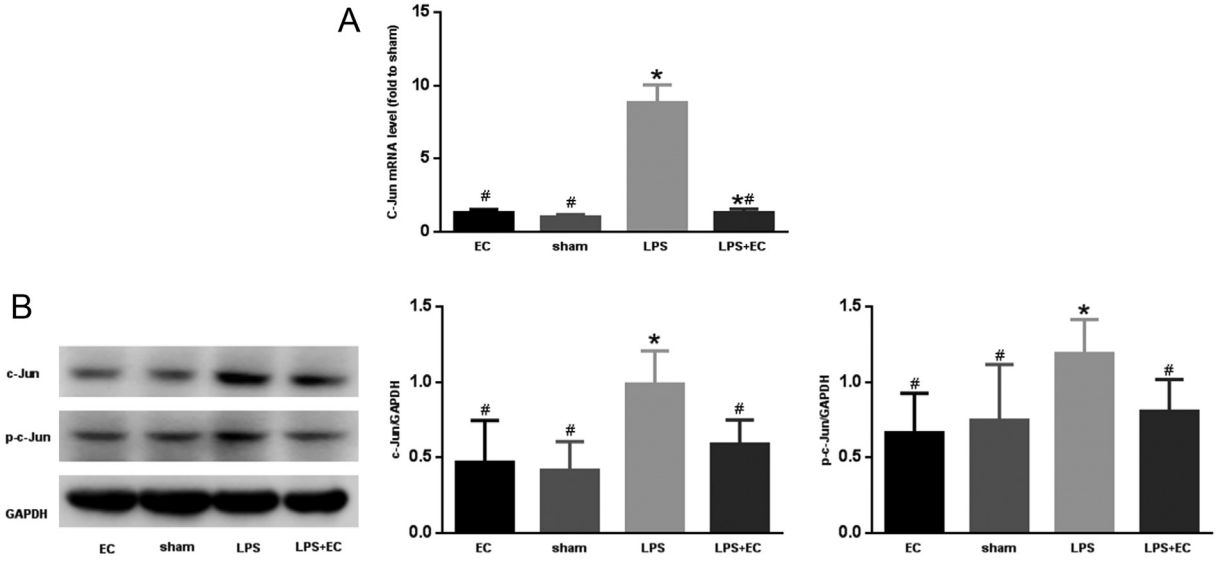

Fig. 6. Epicatechin suppresses the expression and activation of c-Jun in the lungs of mice with LPS-induced ALI. (A) qRT-PCR analysis of c-Jun mRNA levels in lung tissue collected at 24 h after the indicated treatments. (B) Western blot analysis (left) and quantification (right) of total c-Jun and phosphorylated c-Jun (p-c-Jun) protein levels in lung tissue collected at 24 h after the indicated treatments. Values are the mean ± SD of 8 mice/group. *$P < 0.05$ vs. the sham group, #$P < 0.05$ vs. the LPS group.

relevant to this article.

References

[1] G.R. Bernard, Acute respiratory distress syndrome: a historical perspective[J], Am. J. Respir. Crit. Care Med. 172 (7) (2005) 798–806.

[2] L.P. Zhang, Y. Zhao, G.J. Liu, et al., Glabridin attenuates lipopolysaccharide-induced acute lung injury by inhibiting p38MAPK/ERK signaling pathway[J], Oncotarget 8 (12) (2017) 18935–18942.

[3] J.R. Park, H. Lee, S.I. Kim, et al., The tri-peptide GHK-Cu complex ameliorates lipopolysaccharide-induced acute lung injury in mice[J], Oncotarget 7 (36) (2016) 58405–58417.

[4] G. Matute-Bello, C.W. Frevert, T.R. Martin, Animal models of acute lung injury[J], Am. J. Phys. Lung Cell. Mol. Phys. 295 (3) (2008) L379–L399.

[5] B. Beutler, Tlr4: central component of the sole mammalian LPS sensor[J], Curr. Opin. Immunol. 12 (1) (2000) 20–26.

[6] P.C. Vasconcelos, L.N. Seito, L.C. Di Stasi, et al., Epicatechin used in the treatment of intestinal inflammatory disease: an analysis by experimental models[J], Evid. Based Complement. Alternat. Med. 2012 (2012) 508902.

[7] I. Andujar, M.C. Recio, R.M. Giner, et al., Inhibition of ulcerative colitis in mice after oral administration of a polyphenol-enriched cocoa extract is mediated by the inhibition of STAT1 and STAT3 phosphorylation in colon cells[J], J. Agric. Food Chem. 59 (12) (2011) 6474–6483.

[8] M. Iranshahi, R. Rezaee, H. Parhiz, et al., Protective effects of flavonoids against microbes and toxins: the cases of hesperidin and hesperetin[J], Life Sci. 137 (2015) 125–132.

[9] J. Xing, R. Li, N. Li, et al., Anti-inflammatory effect of procyanidin B1 on LPS-treated THP1 cells via interaction with the TLR4-MD-2 heterodimer and p38 MAPK and NF-kappaB signaling[J], Mol. Cell. Biochem. 407 (1–2) (2015) 89–95.

[10] A. Bettaieb, M.A. Vazquez Prieto, C. Rodriguez Lanzi, et al., (−)-Epicatechin mitigates high-fructose-associated insulin resistance by modulating redox signaling and endoplasmic reticulum stress[J], Free Radic. Biol. Med. 72 (2014) 247–256.

[11] P.D. Prince, L. Fischerman, J.E. Toblli, et al., LPS-induced renal inflammation is prevented by (−)-epicatechin in rats[J], Redox Biol. 11 (2017) 342–349.

[12] E.J. Ruijters, G.R. Haenen, A.R. Weseler, et al., The cocoa flavanol (−)-epicatechin protects the cortisol response[J], Pharmacol. Res. 79 (2014) 28–33.

[13] C.F. Chang, S. Cho, J. Wang, (−)-Epicatechin protects hemorrhagic brain via synergistic Nrf2 pathways[J], Ann. Clin. Transl. Neurol. 1 (4) (2014) 258–271.

[14] C.J. Cox, F. Choudhry, E. Peacey, et al., Dietary (−)-epicatechin as a potent inhibitor of betagamma-secretase amyloid precursor protein processing[J], Neurobiol. Aging 36 (1) (2015) 178–187.

[15] L. Wu, Q.L. Zhang, X.Y. Zhang, et al., Pharmacokinetics and blood-brain barrier penetration of (+)-catechin and (−)-epicatechin in rats by microdialysis sampling coupled to high-performance liquid chromatography with chemiluminescence detection[J], J. Agric. Food Chem. 60 (37) (2012) 9377–9383.

[16] R.J. Bennink, W.J. De Jonge, E.L. Symonds, et al., Validation of gastric-emptying scintigraphy of solids and liquids in mice using dedicated animal pinhole scintigraphy[J], J. Nucl. Med. 44 (7) (2003) 1099–1104.

[17] T. Cheng, W. Wang, Q. Li, et al., Cerebroprotection of flavanol (−)-epicatechin after traumatic brain injury via Nrf2-dependent and -independent pathways[J], Free Radic. Biol. Med. 92 (2016) 15–28.

[18] G. Matute-Bello, G. Downey, B.B. Moore, et al., An official American Thoracic Society workshop report: features and measurements of experimental acute lung injury in animals[J], Am. J. Respir. Cell Mol. Biol. 44 (5) (2011) 725–738.

[19] X. Chen, F.J. Walther, R.M. Sengers, et al., Metformin attenuates hyperoxia-induced lung injury in neonatal rats by reducing the inflammatory response[J], Am. J. Phys. Lung Cell. Mol. Phys. 309 (3) (2015) L262–L270.

[20] B. Baur, K. Storch, K.E. Martz, et al., Metabolically stable dibenzo[b,e]oxepin-11(6H)-ones as highly selective p38 MAP kinase inhibitors: optimizing anti-cytokine activity in human whole blood[J], J. Med. Chem. 56 (21) (2013) 8561–8578.

[21] A. Singh, A. Demont, L. Actis-Goretta, et al., Identification of epicatechin as one of the key bioactive constituents of polyphenol-enriched extracts that demonstrate an anti-allergic effect in a murine model of food allergy[J], Br. J. Nutr. 112 (3) (2014) 358–368.

[22] C.G. Fraga, P.I. Oteiza, Dietary flavonoids: Role of (−)-epicatechin and related procyanidins in cell signaling[J], Free Radic. Biol. Med. 51 (4) (2011) 813–823.

[23] G.G. Mackenzie, F. Carrasquedo, J.M. Delfino, et al., Epicatechin, catechin, and dimeric procyanidins inhibit PMA-induced NF-kappaB activation at multiple steps in Jurkat T cells[J], FASEB J. 18 (1) (2004) 167–169.

[24] T.R. Martin, Neutrophils and lung injury: getting it right[J], J. Clin. Invest. 110 (11) (2002) 1603–1605.

[25] H.J. Kim, H.S. Lee, Y.H. Chong, et al., p38 Mitogen-activated protein kinase up-regulates LPS-induced NF-kappaB activation in the development of lung injury and RAW 264.7 macrophages[J], Toxicology 225 (1) (2006) 36–47.

[26] X. Liu, B. Ma, A.B. Malik, et al., Bidirectional regulation of neutrophil migration by mitogen-activated protein kinases[J], Nat. Immunol. 13 (5) (2012) 457–464.

[27] S. Schnyder-Candrian, V.F. Quesniaux, F. Di Padova, et al., Dual effects of p38 MAPK on TNF-dependent bronchoconstriction and TNF-independent neutrophil recruitment in lipopolysaccharide-induced acute respiratory distress syndrome[J], J. Immunol. 175 (1) (2005) 262–269.

[28] L. Wang, M.H. Pan, C.Y. Lo, et al., Anti-fibrotic activity of polyphenol-enriched sugarcane extract in rats via inhibition of p38 and JNK phosphorylation[J], Food Funct. 9 (2) (2018) 951–958.

[29] M.A. Vazquez-Prieto, A. Bettaieb, F.G. Haj, et al., (−)-Epicatechin prevents TNFalpha-induced activation of signaling cascades involved in inflammation and insulin sensitivity in 3T3-L1 adipocytes[J], Arch. Biochem. Biophys. 527 (2) (2012) 113–118.

[30] P.I. Oteiza, C.G. Fraga, D.A. Mills, et al., Flavonoids and the gastrointestinal tract: local and systemic effects[J], Mol. Asp. Med. 61 (2018) 41–49.

[31] T. Zarubin, J. Han, Activation and signaling of the p38 MAP kinase pathway[J], Cell Res. 15 (1) (2005) 11–18.

[32] M. Karin, The regulation of AP-1 activity by mitogen-activated protein kinases[J], Philos. Trans. R. Soc. Lond. Ser. B Biol. Sci. 351 (1336) (1996) 127–134.

[33] A. Bhoumik, P. Lopez-Bergami, Z. Ronai, ATF2 on the double - activating transcription factor and DNA damage response protein[J], Pigment Cell Res. 20 (6) (2007) 498–506.